

# Hydrodynamic fluctuations of entropy in one-dimensionally expanding system

Tetsufumi Hirano<sup>a</sup>, Ryuichi Kurita<sup>b</sup>, Koichi Murase<sup>a</sup>

<sup>a</sup>*Department of Physics, Sophia University, Tokyo 102-8554, Japan*

<sup>b</sup>*Department of Physics, The University of Tokyo, Hongo 7-3-1, Bunkyo-ku, Tokyo 113-0033, Japan*

---

## Abstract

The fluctuation-dissipation relation tells that dissipation always accompanies with thermal fluctuations. Relativistic fluctuating hydrodynamics is used to study the effects of the thermal fluctuations in the hydrodynamic expansion of the quark-gluon plasma created in the high-energy nuclear collisions. We show that the thermal noise obeys the steady-state fluctuation theorem when (i) the time scales of the evolution of thermodynamic quantities are sufficiently longer than the relaxation time, and (ii) the thermal fluctuations of temperature are sufficiently small. The steady-state fluctuation theorem describes the distribution of the entropy which can be related to the multiplicity observed in high-energy nuclear collisions. As a consequence, we propose an upper bound to the multiplicity fluctuations which is useful to test the initial state models. We also numerically investigate breaking of the steady-state fluctuation theorem due to the non-vanishing relaxation time in real nuclear collisions.

---

## 1. Introduction

Under extremely hot and/or dense circumstance, quarks and gluons inside hadrons are deconfined to form quark-gluon plasma (QGP). The QGP can be created experimentally in high-energy nuclear collisions at Relativistic Heavy Ion Collider (RHIC) in Brookhaven National Laboratory and at Large Hadron Collider (LHC) in CERN. Just after RHIC started its operation, relativistic ideal hydrodynamics turned out to work reasonably well for the description of the spacetime evolution of the QGP [1, 2, 3]. Simulations of relativistic dissipative hydrodynamics have been extensively performed so far towards further quantitative understanding of the transport properties of the QGP [4, 5]. Detailed hydrodynamic studies indicate the ratio of shear viscosity to entropy density in the QGP is very small [6, 7, 8].

In the past years, various kinds of fluctuations have attracted a lot of theoretical and experimental attention. Observed higher harmonics of azimuthal anisotropy [9, 10, 11, 12, 13] is explained by initial fluctuations of the transverse profile of the QGP [14]. Hydrodynamic responses of the QGP to the initial fluctuations give a reasonable interpretation of the higher harmonics. Another example is the analysis of fluctuations of conserved charges which could be used to find the signal of quantum chromodynamics (QCD) critical point where the phase transition from the QGP to hadrons is the second-order one [15, 16].

The fluctuations to be addressed in this paper are thermal fluctuations appearing in hydrodynamics. Thermal equilibrium is a state of maximum entropy in a macro-

scopic sense. However, the system is always microscopically fluctuating due to the thermal noises, *i.e.*, the thermodynamic variables slightly deviate from their expectation values on an event-by-event basis in the thermal equilibrium state. This process reduces the entropy of the system. At the same time, the system relaxes to the equilibrium state due to the dissipation, which generates the entropy. These two processes are compensated with each other for the system to be stable and to maintain the entropy around its maximum. The relation that holds between these two is called the fluctuation-dissipation relation (FDR). In the hydrodynamic language, the dissipative currents, such as the shear stress and the diffusion currents, are driven by systematic forces (thermodynamic forces) and, at the same time, random forces (hydrodynamic fluctuations) on an event-by-event basis. In the hydrodynamic description of high-energy nuclear collision process, while the dissipative effects such as shear viscosity have been taken into account, the effects of hydrodynamic fluctuations have not been widely discussed. However, in a viewpoint of the fluctuation-dissipation theorem, both effects should be consistently discussed together. In this paper, employing a relativistic version of second-order fluctuating hydrodynamics [17], we investigate the fluctuations of entropy production under longitudinally boost-invariant (Bjorken) expansion [18] in high-energy nuclear collisions.

In many years, the linear response theory [19] has been the milestone in non-equilibrium statistical mechanics. On the other hand, in these years, the *fluctuation theorem* [20, 21, 22] has been established to quantify production of entropy of the system away from equilibrium. Since the theorem includes the FDR in the system close to equilibrium, it is often regarded as a general framework to analyse the dynamical system even far from equilibrium. In this

---

*Email addresses:* hirano@sophia.ac.jp (Tetsufumi Hirano), murase@sophia.ac.jp (Koichi Murase)

paper, we discuss the fluctuation theorem in the context of the physics of high-energy nuclear collisions for the first time.

The paper is organised as follows: In Sec. 2, we briefly introduce relativistic fluctuating hydrodynamics and apply it to longitudinally boost-invariant expansion. First we show that the steady-state fluctuation theorem exactly holds for the hydrodynamic system under some idealised limits in Sec. 3. In Sec. 4, we discuss the consequence in the observables of high-energy nuclear collisions. In particular we obtain an upper bound of the power of final-entropy fluctuations and discuss a consequence to the experimental multiplicities. Next, in Sec. 5, we perform numerical simulations of the Bjorken expansion to quantify the breaking of the steady-state fluctuation theorem in a realistic condition. In Sec. 6, we discuss two effects breaking the steady-state fluctuation theorem, *i.e.*, the finite relaxation time and the fluctuations of the temperature caused by the hydrodynamic fluctuations. Finally Sec. 7 is devoted to the conclusion.

In this paper, we employ natural units,  $c = \hbar = k_B = 1$ , and the Minkowski metric,  $g_{\mu\nu} = \text{diag}(1, -1, -1, -1)$ .

## 2. Relativistic fluctuating hydrodynamics in Bjorken expansion

In this section we review relativistic fluctuating hydrodynamics and obtain the expression of the FDR in the Bjorken expansion.

Hydrodynamic equations are the continuity equation for energy and momentum,

$$\partial_\mu T^{\mu\nu} = 0. \quad (1)$$

The energy-momentum tensor  $T^{\mu\nu}$  in the Landau (energy) frame is written down as

$$T^{\mu\nu} = e u^\mu u^\nu - (p + \Pi) \Delta^{\mu\nu} + \pi^{\mu\nu}, \quad (2)$$

where  $e$ ,  $p$ ,  $\pi^{\mu\nu}$  and  $\Pi$  are the energy density, the equilibrium pressure, the shear stress tensor and the bulk pressure, respectively. In this paper we do not consider the other conserved currents. The tensor  $\Delta^{\mu\nu} = g^{\mu\nu} - u^\mu u^\nu$  is the projector onto the space perpendicular to the four-flow velocity  $u^\mu$ . To close Eq. (1), one needs the assumption on the equation of state  $p = p(e)$  and the constitutive equations for the dissipative currents,  $\pi^{\mu\nu}$  and  $\Pi$ . In relativistic fluctuating hydrodynamics, the second-order constitutive equations can be written as stochastic equations [17]:

$$\tau_\pi \Delta^{\mu\nu}{}_{\alpha\beta} D \pi^{\alpha\beta} + \pi^{\mu\nu} = 2\eta \Delta^{\mu\nu}{}_{\alpha\beta} \partial^\alpha u^\beta + \xi^{\mu\nu}, \quad (3)$$

$$(\tau_\Pi D + 1) \Pi = -\zeta \theta + \xi, \quad (4)$$

where transport coefficients  $\eta$  ( $\zeta$ ) and  $\tau_\pi$  ( $\tau_\Pi$ ) are the shear (bulk) viscosity and the relaxation time for the shear stress tensor (bulk pressure), respectively. The tensor  $\Delta^{\mu\nu\alpha\beta} = \frac{1}{2}(\Delta^{\mu\alpha} \Delta^{\nu\beta} + \Delta^{\mu\beta} \Delta^{\nu\alpha}) - \frac{1}{3} \Delta^{\mu\nu} \Delta^{\alpha\beta}$  is a projector for second rank tensors onto the symmetric and traceless components

transverse to the flow velocity. The operator  $D = u_\alpha \partial^\alpha$  is the time derivative along the flow velocity, and  $\theta = \partial_\alpha u^\alpha$  is the expansion scalar. The noise terms  $\xi^{\mu\nu}$  and  $\xi$  are the hydrodynamic fluctuations of the shear stress and bulk pressure, respectively, whose intensities are given by the FDR [17]:

$$\langle \xi^{\mu\nu}(x) \xi^{\alpha\beta}(x') \rangle = 4T\eta \Delta^{\mu\nu\alpha\beta} \delta^{(4)}(x - x'), \quad (5)$$

$$\langle \xi(x) \xi(x') \rangle = 2T\zeta \delta^{(4)}(x - x'), \quad (6)$$

where  $\langle O \rangle$  denotes the average with respect to the hydrodynamic fluctuations.

In the Bjorken expansion [18], the flow velocity is given by  $u^\mu = (t/\tau, 0, 0, z/\tau) = (\cosh \eta_s, 0, 0, \sinh \eta_s)$ , where  $\tau = \sqrt{t^2 - z^2}$  and  $\eta_s = (1/2) \ln[(t+z)/(t-z)]$  are the proper time and the spacetime rapidity, respectively. The energy-momentum conservation (1) is reduced to the time evolution of energy density,

$$\frac{de}{d\tau} = -\frac{e+p}{\tau} \left( 1 - \frac{\pi - \Pi}{sT} \right), \quad (7)$$

where  $s = (e+p)/T$  is the entropy density and  $\pi = \pi^{00} - \pi^{33}$ . From Eqs. (3) and (4), we obtain the following constitutive equations for  $\pi$  and  $\Pi$ :

$$\left( \tau_\pi \frac{d}{d\tau} + 1 \right) \pi = \frac{4\eta}{3T} + \xi_\pi, \quad (8)$$

$$\left( \tau_\Pi \frac{d}{d\tau} + 1 \right) \Pi = -\frac{\zeta}{\tau} + \xi_\Pi. \quad (9)$$

Here, to properly define the noise terms, we need to introduce a ‘‘fluid element’’, that we observe, with the expanding volume of  $\tau \Delta \eta_s \Delta x \Delta y$  with  $\Delta \eta_s$ ,  $\Delta x$  or  $\Delta y$  being the length of the fluid element in each direction. The noise terms  $\xi_\pi = \bar{\xi}^{00} - \bar{\xi}^{33}$  and  $\xi_\Pi = \bar{\xi}$  are hydrodynamic fluctuations for  $\pi$  and  $\Pi$ , where  $\bar{\xi}^{\mu\nu}$  and  $\bar{\xi}$  denote the volume average of  $\xi^{\mu\nu}(x)$  and  $\xi(x)$  within the fluid element, respectively. Note that in general the hydrodynamic fluctuations arise independently at each spacetime point to induce inhomogeneity, which would eventually break the boost-invariant expansion of the system, but here we neglect such effects by assuming the fluctuation-induced flow is small enough compared to the Bjorken flow. According to the fluctuation-dissipation relations (5) and (6), these hydrodynamic noises satisfy the statistical properties,

$$\langle \xi_\pi(\tau) \xi_\pi(\tau') \rangle = \frac{8T\eta}{3\tau \Delta \eta_s \Delta x \Delta y} \delta(\tau - \tau'), \quad (10)$$

$$\langle \xi_\Pi(\tau) \xi_\Pi(\tau') \rangle = \frac{2T\zeta}{\tau \Delta \eta_s \Delta x \Delta y} \delta(\tau - \tau'). \quad (11)$$

When the system is close to the local equilibrium, the noise terms,  $\xi_\pi$  and  $\xi_\Pi$ , have Gaussian distributions. Once models for the equation of state and transport coefficients (including relaxation time) are specified, one can solve the stochastic hydrodynamic equations (7) and (8), combined with noises following Eqs. (10) and (11), as an initial value

problem with a given initial condition. We note that there are two interpretations of the stochastic differential equations, the Itô integral and the Stratonovich integral. Here we employ the latter one for the stochastic differential equations in this paper.

### 3. Steady-state fluctuation theorem in the Bjorken expansion

We first introduce the fluctuation theorem (FT) [20, 21, 22]. The FT is a relation on the distribution of entropy production in non-equilibrium processes, which has been proven in various types of systems. The amount of entropy production can generally fluctuate from event to event due to thermal fluctuations even if an initial condition is fixed in a macroscopic sense since a macroscopic state contains ensemble of different microscopic states. The steady-state fluctuation theorem (SSFT), which is a certain version of the FT, gives a relation between two probabilities in stationary processes:

$$\ln \frac{P(\bar{\sigma} = \alpha)}{P(\bar{\sigma} = -\alpha)} = \alpha t, \quad (t/t_R \gg 1), \quad (12)$$

where  $\sigma$  is entropy production rate,  $\bar{\sigma}$  is its time average,  $t$  is the observation time, and  $t_R$  is the relaxation time scale which characterises the stationary process. The function  $P(\bar{\sigma})$  denotes probability density that the specified average entropy production rate is realised. Here it should be emphasised that the entropy can even decrease at a short time scale at small probability through non-equilibrium processes. In a strict sense, the SSFT cannot be applied to the Bjorken expansion because it is not a stationary process. However, if the expansion time scale is sufficiently longer than the microscopic time scale  $t_R$ , we would expect that the SSFT appears as an approximate relation also in the Bjorken expansion.

Here we should note that there is a more general version of the FT, which can be applied to non-stationary processes, called the transient fluctuation theorem (TFT) which gives the following relation:

$$\ln \frac{P(\bar{\sigma} = \alpha)}{P^\dagger(\bar{\sigma}^\dagger = -\alpha)} = \alpha t, \quad (13)$$

where  $P(\bar{\sigma})$  and  $P^\dagger(\bar{\sigma}^\dagger)$  denote the probability densities that the specified average entropy production rate is realised in the considered process and its corresponding time-reversal process, respectively. Applying the TFT to the Bjorken expansion, we might obtain a relation between probabilities of the Bjorken expansion and its time-reversal process, *i.e.*, the one-dimensional compression. However, in high-energy nuclear collisions, such relativistic compression of thermalised matter cannot be realised experimentally, and therefore it is difficult to relate the TFT to experimental observables. For this reason we focus on the SSFT rather than the TFT in this paper.

To discuss the FT in the Bjorken expansion, we shall first define the entropy production rate in the fluid element of the volume  $\tau \Delta \eta_s \Delta x \Delta y$  as

$$\begin{aligned} \sigma &= \frac{d}{d\tau} (s\tau \Delta \eta_s \Delta x \Delta y) \\ &= \frac{\pi - \Pi}{T} \Delta \eta_s \Delta x \Delta y, \end{aligned} \quad (14)$$

where we used Eq. (7) and a thermodynamic relation,  $ds = de/T$ , to obtain the second line. We note that  $s\tau \Delta \eta_s \Delta x \Delta y = (s\gamma)(\tau \Delta \eta_s \Delta x \Delta y / \gamma)$  is a Lorentz-invariant combination with  $\gamma = u^0$  being the Lorentz factor. The average entropy production rate,  $\bar{\sigma}$ , in a time duration from the initial time  $\tau_i$  to the current time  $\tau$  is written as

$$\bar{\sigma} = \frac{1}{\tau - \tau_i} \int_{\tau_i}^{\tau} d\tau' \frac{\pi(\tau') - \Pi(\tau')}{T(\tau')} \Delta \eta_s \Delta x \Delta y, \quad (15)$$

where  $\pi(\tau)$  and  $\Pi(\tau)$  are formally given by solving Eqs. (8) and (9):

$$\pi(\tau) = \int_{\tau_i}^{\tau} d\tau' G_\pi(\tau, \tau') \frac{4\eta(\tau')}{3\tau'} + \delta\pi(\tau), \quad (16)$$

$$\Pi(\tau) = - \int_{\tau_i}^{\tau} d\tau' G_\Pi(\tau, \tau') \frac{\zeta(\tau')}{\tau'} + \delta\Pi(\tau), \quad (17)$$

$$G_{\pi/\Pi}(\tau_2, \tau_1) = \exp \left[ - \int_{\tau_1}^{\tau_2} \frac{d\tau}{\tau_{\pi/\Pi}(\tau)} \right] \frac{1}{\tau_{\pi/\Pi}(\tau_1)}. \quad (18)$$

Here we ignore the terms that depend on the initial values,  $\pi(\tau_i)$  and  $\Pi(\tau_i)$ , because these terms damp to vanish when  $\tau - \tau_i \gg \tau_{\pi/\Pi}$ . The time dependence of the transport coefficients,  $\eta(\tau)$ ,  $\zeta(\tau)$  and  $\tau_{\pi/\Pi}(\tau)$ , comes from the time evolution of temperature  $T(\tau)$ . The fluctuation parts,  $\delta\pi(\tau)$  and  $\delta\Pi(\tau)$ , are accumulated noises of  $\xi_\pi$  and  $\xi_\Pi$ , respectively:

$$\delta\pi(\tau) = \int_{\tau_i}^{\tau} d\tau' G_\pi(\tau, \tau') \xi_\pi(\tau'), \quad (19)$$

$$\delta\Pi(\tau) = \int_{\tau_i}^{\tau} d\tau' G_\Pi(\tau, \tau') \xi_\Pi(\tau'). \quad (20)$$

Next we consider the following two idealised conditions:

(i) the considered volume is sufficiently large so that the change of the background temperature caused by fluctuations is negligible, and (ii) the relaxation times,  $\tau_\pi$  and  $\tau_\Pi$ , are sufficiently shorter than the variation time scale of the temperature and the thermodynamic forces, *i.e.*, the Navier–Stokes limit  $\tau_{\pi/\Pi} \rightarrow 0$  can be safely taken.

Under the condition (ii), the Green function (18) is reduced to the delta function  $\delta(\tau)$ , and the first terms in the right-hand sides of Eqs. (16) and (17) become the Navier–Stokes (first-order) terms. The integrated noises,  $\delta\pi(\tau)$  and  $\delta\Pi(\tau)$ , are reduced to  $\xi_\pi(\tau)$  and  $\xi_\Pi(\tau)$ , respectively, so their correlations are simply given by Eqs. (10) and (11). For the condition (i), we first define the background  $T_0(\tau)$  as the time evolution of the temperature without noises that is obtained by solving Eqs. (7)–(9) with  $\xi_\pi = \xi_\Pi = 0$ .

Using the condition (i), the temperature and the transport coefficients in the expression of the entropy production rate can be replaced by their background values,  $T_0(\tau)$ ,  $\eta_0(\tau) = \eta(T_0(\tau))$  and  $\zeta_0(\tau) = \zeta(T_0(\tau))$ , to obtain the following expression:

$$\bar{\sigma} = \frac{\Delta\eta_s \Delta x \Delta y}{\tau - \tau_i} \int_{\tau_i}^{\tau} \frac{d\tau'}{T_0(\tau')} \times \left[ \frac{4\eta_0(\tau')}{3\tau'} + \frac{\zeta_0(\tau')}{\tau'} + \xi_{\pi}(\tau') - \xi_{\Pi}(\tau') \right]. \quad (21)$$

In this expression we notice that the fluctuations contribute to the entropy production only at the linear order, and thus the resulting distribution of the entropy production rate becomes a Gaussian one. Here we calculate the mean and the variance that characterise the Gaussian distribution of the entropy production rate:

$$\begin{aligned} \langle \bar{\sigma} \rangle &= \frac{\Delta\eta_s \Delta x \Delta y}{\tau - \tau_i} \int_{\tau_i}^{\tau} \frac{d\tau'}{T_0(\tau')} \left[ \frac{4\eta_0(\tau')}{3\tau'} + \frac{\zeta_0(\tau')}{\tau'} \right], \quad (22) \\ a^2 &= \langle \bar{\sigma}^2 \rangle - \langle \bar{\sigma} \rangle^2 \\ &= \left( \frac{\Delta\eta_s \Delta x \Delta y}{\tau - \tau_i} \right)^2 \int_{\tau_i}^{\tau} d\tau' \int_{\tau_0}^{\tau} d\tau'' \\ &\quad \times \frac{\langle \xi_{\pi}(\tau') \xi_{\pi}(\tau'') \rangle + \langle \xi_{\Pi}(\tau') \xi_{\Pi}(\tau'') \rangle}{T_0(\tau') T_0(\tau'')} \\ &= \frac{2\Delta\eta_s \Delta x \Delta y}{(\tau - \tau_i)^2} \int_{\tau_i}^{\tau} \frac{d\tau'}{T_0(\tau')} \left[ \frac{4\eta_0(\tau')}{3\tau'} + \frac{\zeta_0(\tau')}{\tau'} \right]. \quad (23) \end{aligned}$$

The above expressions of the mean and variance have the same integral structure, and in fact we find the following relation:

$$\frac{2\langle \bar{\sigma} \rangle}{a^2} = \tau - \tau_i. \quad (24)$$

Using this relation, we obtain a version of the SSFT in relativistic fluctuating hydrodynamics in the Bjorken expansion:

$$\ln \frac{P(\bar{\sigma} = \alpha)}{P(\bar{\sigma} = -\alpha)} = \ln \frac{\exp[-(\alpha - \langle \bar{\sigma} \rangle)^2 / 2a^2]}{\exp[-(-\alpha - \langle \bar{\sigma} \rangle)^2 / 2a^2]} \quad (25)$$

$$\begin{aligned} &= \alpha \cdot \frac{2\langle \bar{\sigma} \rangle}{a^2} \\ &= \alpha \cdot (\tau - \tau_i). \quad (26) \end{aligned}$$

We note that, in the above expression, the time duration is measured by the proper time,  $\tau$ , unlike the case of the normal SSFT which is measured by the laboratory time,  $t$ . This is just because the average entropy production rate (15) is defined by the entropy production per unit proper time, and there is no essential difference to the normal SSFT.

#### 4. Upper bound of entropy fluctuations

The entropy distribution can be related to the multiplicity distribution in the high-energy nuclear collisions

since the entropy is approximately proportional to the final multiplicity. In this section we discuss multiplicity fluctuations through entropy fluctuations in the Bjorken expansion described in the previous section. In particular, we show the transverse area dependence of entropy fluctuations and its upper bound.

To quantify the entropy fluctuations, we take a ratio of the standard deviation to the mean value of the entropy distribution at time  $\tau$ , where  $\tau$  is the time at which entropy becomes no longer produced due to the freeze-out process of high-energy nuclear collisions. For one fluid element, the final entropy is  $S(\tau) = S_i + \bar{\sigma}(\tau - \tau_i)$ , and its standard deviation is  $\Delta S(\tau) = a(\tau - \tau_i)$ . By taking an ensemble average for a fixed initial entropy and using Eq. (24), we obtain the ratio,

$$\begin{aligned} \frac{\Delta S(\tau)}{\langle S(\tau) \rangle} &= \frac{a(\tau - \tau_i)}{S_i + \langle \bar{\sigma} \rangle (\tau - \tau_i)} \\ &= \frac{\sqrt{2\langle \bar{\sigma} \rangle (\tau - \tau_i)}}{S_i + \langle \bar{\sigma} \rangle (\tau - \tau_i)} \\ &= \frac{\sqrt{2\langle \delta(\tau s) \rangle}}{\tau_i s_i + \langle \delta(\tau s) \rangle} \frac{1}{\sqrt{\Delta\eta_s \Delta x \Delta y}}, \quad (27) \end{aligned}$$

where  $\delta(\tau s) = \tau s - \tau_i s_i$ , and  $s_i$  is the initial entropy density. In the second line we used the fact that the entropy in one fluid element is written as  $S = \tau s \Delta\eta_s \Delta x \Delta y$ . An entire collision system is considered to be a set of fluid elements, so we estimate the number of fluid elements in the transverse plane,  $n$ , from the transverse area of the system,  $A$ , as

$$n = \frac{A}{\Delta x \Delta y}. \quad (28)$$

From the assumption of hydrodynamics that each fluid element can be approximated as a local-equilibrium system, fluctuations of each fluid element are considered to be statistically independent. Therefore the relative fluctuations of the total entropy  $\Delta S_{\text{tot}}$  in the rapidity range  $\Delta\eta_s$  are obtained as

$$\begin{aligned} \frac{\Delta S_{\text{tot}}}{\langle S_{\text{tot}} \rangle} &= \frac{1}{\sqrt{n}} \frac{\Delta S(\tau)}{\langle S(\tau) \rangle} \\ &= \frac{\sqrt{2\langle \delta(\tau s) \rangle}}{\tau_i s_i + \langle \delta(\tau s) \rangle} \frac{1}{\sqrt{A \Delta\eta_s}}. \quad (29) \end{aligned}$$

The proportionality,  $\Delta S_{\text{tot}} / S_{\text{tot}} \propto 1 / \sqrt{A \Delta\eta_s}$ , is the common scaling of the relative fluctuations of macroscopic variables with respect to the system size. Here we can identify  $\sqrt{2\langle \delta(\tau s) \rangle} / (\tau_i s_i + \langle \delta(\tau s) \rangle)$  as the constant of the proportionality. From this proportionality we can say that the effects of thermal fluctuations are more significant in smaller systems, such as  $p$ -A or very peripheral A-A collisions, if hydrodynamics works in such small systems.

Moreover from Eq. (29), we can find an upper bound of the entropy fluctuations:

$$\frac{\Delta S_{\text{tot}}}{\langle S_{\text{tot}} \rangle} \leq \frac{1}{\sqrt{2\tau_i s_i}} \frac{1}{\sqrt{A \Delta\eta_s}} = \frac{1}{\sqrt{2S_{\text{tot},i}}}, \quad (30)$$

where  $S_{\text{tot},i} = \tau_i s_i A \Delta \eta_s$  is the initial total entropy in the rapidity range. To obtain the inequality, we used a mathematical inequality  $\frac{\sqrt{2x}}{a+x} \leq \frac{1}{\sqrt{2a}}$  for  $x \geq 0$  and any positive constant  $a$ , where the equality is satisfied in the case  $x = a$ . The most important point is that the upper bound of the entropy fluctuations is solely determined by the initial total entropy  $S_{\text{tot},i}$  and does not depend on the details of the intermediate dynamics such as the equation of state and the value of transport coefficients. We also note that the upper bound is independent of the fluid element size,  $\tau \Delta \eta_s \Delta x \Delta y$ , which we assumed in the derivation.

Equation (30) is the inequality for a fixed initial condition with the total entropy  $S_{\text{tot},i}$ . To relate the Eq. (30) to the experimental multiplicities, we need to consider event averages over initial conditions. Here we make two simplifications that both of  $S_{\text{tot},i}$  and  $\langle S_{\text{tot}} \rangle$  are proportional to the transverse area  $A$ , and that the multiplicity distribution for a fixed final entropy  $S_{\text{tot}}$  follows the Poisson distribution. Using these simplifications we can find an upper bound of the multiplicity fluctuations as follows (see Appendix A for the derivation):

$$\frac{(\Delta_{\text{ev}} N)^2 - \langle N \rangle_{\text{ev}}}{\langle N \rangle_{\text{ev}}^2} \leq \frac{(\Delta_{\text{ev}} S_{\text{tot},i})^2}{\langle S_{\text{tot},i} \rangle_{\text{ev}}^2} + \frac{1}{2 \langle S_{\text{tot},i} \rangle_{\text{ev}}}, \quad (31)$$

where  $N$  is the multiplicity in a considered rapidity range,  $\langle N \rangle_{\text{ev}}$  and  $\langle S_{\text{tot},i} \rangle_{\text{ev}}$  are the event averages of  $N$  and the initial entropy  $S_{\text{tot},i}$ , and  $(\Delta_{\text{ev}} N)^2 = \langle (N - \langle N \rangle_{\text{ev}})^2 \rangle_{\text{ev}}$  and  $(\Delta_{\text{ev}} S_{\text{tot},i})^2 = \langle (S_{\text{tot},i} - \langle S_{\text{tot},i} \rangle_{\text{ev}})^2 \rangle_{\text{ev}}$  are the variance of  $N$  and  $S_{\text{tot},i}$ , respectively. The second term in the left-hand side comes from the Poisson statistics. Here one notices that the right-hand side is totally written by the quantities specific to initial conditions, and the left-hand side can be measured in experiments. Therefore this inequality may be used to test initial state models in comparison with experimental data without relying on any specific modeling of intermediate dynamics.

## 5. Numerical tests

In Secs. 3 and 4, we assumed the Navier–Stokes limit where the relaxation time is negligible. A non-vanishing relaxation time is, however, needed to maintain the causality in relativistic dissipative hydrodynamics [23, 24]. In particular, in high-energy nuclear collisions, the relaxation time is comparable to the time scale of the evolution of thermodynamic quantities. In this section, we consider the effects of the non-vanishing relaxation time on the entropy fluctuations by solving the stochastic differential equation numerically.

First we define a parametrised equation of state and transport coefficients. The lattice QCD simulations indicate a crossover from the hadronic matter to the QGP on the temperature axis with vanishing baryon chemical potential [25, 26, 27]. In this study we employ a model equation of state [28] with a crossover, where the entropy

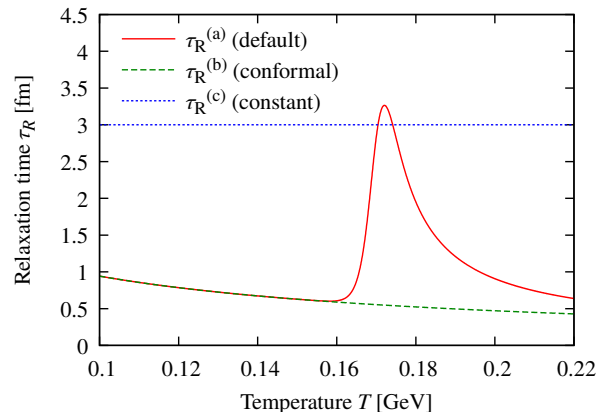


Figure 1: Three models of the relaxation times are shown as functions of temperature. The default relaxation time is shown by the red solid line. The conformal and constant relaxation times are shown by the green dashed and blue dotted lines.

density as a function of temperature is parametrised as

$$s(T) = \frac{4\pi^2}{90} g_h T^3 \frac{1 - \tanh\left(\frac{T-T_c}{d}\right)}{2} + \frac{4\pi^2}{90} g_q T^3 \frac{1 + \tanh\left(\frac{T-T_c}{d}\right)}{2}. \quad (32)$$

Here  $g_h = 3$  and  $g_q = 37$  are degrees of freedom of hadrons and QGP, respectively, in  $N_c = 3$  and  $N_f = 2$  case. In this parametrised form, we can change the crossover temperature  $T_c$  and the crossover region size  $d$  to see their effects, yet for the present study we fix  $T_c = 170$  MeV and  $d = T_c/50$ . Contrary to the equation of state, less known are the transport coefficients of the QGP. Hence, just for the purpose of demonstrating relativistic fluctuating hydrodynamics, we employ the following parametrisation for transport coefficients for the shear and bulk viscosity [29, 30]:

$$\frac{\eta}{s} = \frac{1}{4\pi}, \quad (33)$$

$$\frac{\zeta}{s} = 15 \left( \frac{1}{3} - c_s^2 \right)^2 \frac{\eta}{s}, \quad (34)$$

where  $c_s^2 = dp/de$  is the squared sound velocity. We assume a common relaxation time for the bulk pressure and the shear stress:  $\tau_R = \tau_\pi = \tau_\Pi$ . We mainly consider the relaxation time given by Refs. [31, 32, 33]:

$$\tau_R^{(a)} = \frac{3\eta}{2p}. \quad (35)$$

For the purpose of investigating the effects of the relaxation time on the SSFT, we also consider other models of relaxation times. One is the conformal one,  $\tau_R^{(b)} = 3/2\pi T$ , obtained by applying the equation of state of massless ideal gases to Eq. (35) along with Eq. (33). Another one is a constant relaxation time,  $\tau_R^{(c)} = 3.0$  fm. Figure 1 shows the temperature dependence of the relaxation

times. In the following discussions, the default relaxation time  $\tau_R^{(a)}$  is used if it is not explicitly specified. We choose the initial time  $\tau_i = 1.0$  fm and the initial temperature  $T_i = 0.22$  GeV. The initial values of the dissipative currents are taken to vanish. The size of the fluid element is  $\Delta\eta_s = 1$  and  $\Delta x = \Delta y = 1$  fm. For time integration, we use the second-order stochastic Runge–Kutta method with the strong order 1 (See Appendix B) based on the improved Euler method, for which we choose the time step  $\Delta\tau = 0.1$  fm.

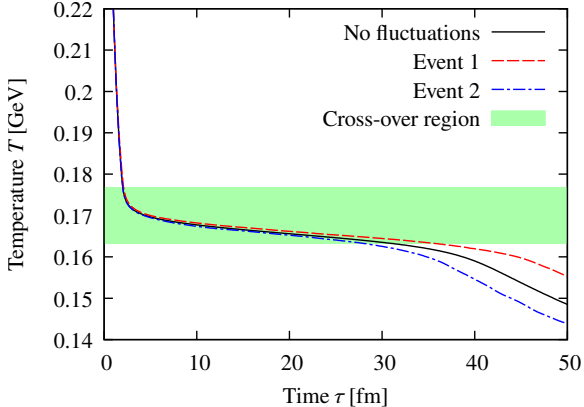


Figure 2: The time evolution of temperature is shown. The black solid line shows the result of dissipative hydrodynamics without fluctuations. The red dashed and blue chain lines are two examples of the results of fluctuating hydrodynamics. The pale green band shows a crossover region  $T \in [T_c - 2d, T_c + 2d]$ .

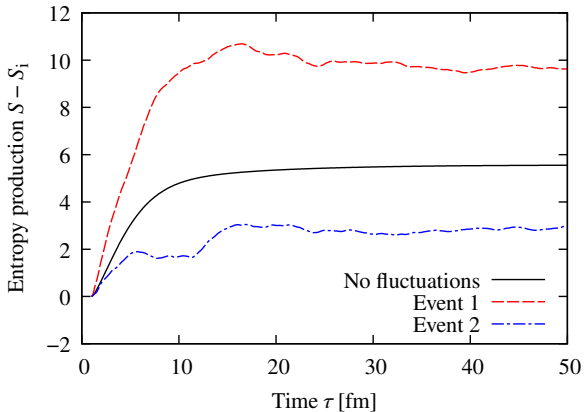


Figure 3: The entropy production in one fluid element,  $S - S_i = \delta(\tau s)\Delta\eta_s\Delta x\Delta y$ , is shown. The black solid line shows the result of dissipative hydrodynamics without fluctuations. The red dashed and blue chain lines are two examples of fluctuating hydrodynamics corresponding to those of Fig. 2.

Figure 2 shows the time evolution of the temperature in dissipative hydrodynamics without fluctuations and two sample events from fluctuating hydrodynamics. One can see that the temperature initially decreases rapidly, goes down slowly in the crossover region, and finally decreases rapidly again after passing through the crossover region at

$\tau \sim 40$ – $50$  fm. Also the temperature difference between dissipative hydrodynamics and fluctuating hydrodynamics is still an order of a few percent after the crossover region  $\tau \sim 50$  fm in typical events as seen in Fig. 2. This means that the condition (i) in Sec. 3 is a good approximation in the current setup.

The entropy production for the fluid element as a function of time is shown in Fig. 3. While the total entropy is conserved in ideal hydrodynamics, it monotonically increases in dissipative hydrodynamics due to the second law of thermodynamics as shown by the solid line. Specifically, the increase is rapid in the early time ( $\tau \lesssim 10$  fm) and slows down afterwards since the dissipative currents appearing in the expression of entropy production (14) are on average proportional to the thermodynamic force which is  $1/\tau$  in the Bjorken expansion. We also show two examples of the entropy production of fluctuating hydrodynamics with dashed and chain lines, which fluctuate around the results of dissipative hydrodynamics. One notices that the fluctuations of the entropy production are more significant compared to the temperature fluctuations (shown in Fig. 2) although the entropy is a function of temperature. This is because the tiny fluctuations of temperature are magnified by the steep change of the entropy in the crossover region. One also observes that entropy can even decrease in short time scales, which can be explained by the fluctuation theorem (12) claiming that the entropy of a small system can decrease in a short time scale with a small, but still non-zero, probability. We note that the second law of thermodynamics corresponds to the fact that the entropy increases on average in fluctuating hydrodynamics.

Using Eq. (14), the temporal decrease of the entropy can be attributed to the behaviours of the bulk pressure  $\Pi$  and shear stress  $\pi$ , which are shown in Fig. 4. These dissipative currents of fluctuating hydrodynamics fluctuate around the ones of dissipative hydrodynamics. We see that, unlike in expanding systems in dissipative hydrodynamics, the bulk pressure (shear stress) can be positive (negative) in fluctuating hydrodynamics, which causes the negative entropy production rate,  $\sigma \propto \pi - \Pi < 0$ .

So far we have discussed the time evolution of fluctuating hydrodynamics using two sample events. Now, to discuss the SSFT in the Bjorken expansion, we perform 10000 events of simulations for each model of the relaxation time and obtain the probability distribution of the entropy production. Figure 5 shows the entropy production distribution in the fluid element at  $\tau = 50$  fm for the three models of the relaxation time. One can observe that there are non-negligible probabilities that the entropy production becomes negative, *i.e.*, the final entropy becomes smaller than the initial value. The probabilities of negative entropy production are 8.42(28)%, 3.41(18)% and 3.70(18)% for  $\tau_R^{(a)}$ ,  $\tau_R^{(b)}$  and  $\tau_R^{(c)}$ , respectively. One can see that for all the relaxation time the distribution is well fitted by Gaussian although each can have quite different mean and variance. This means that the equality (25) in

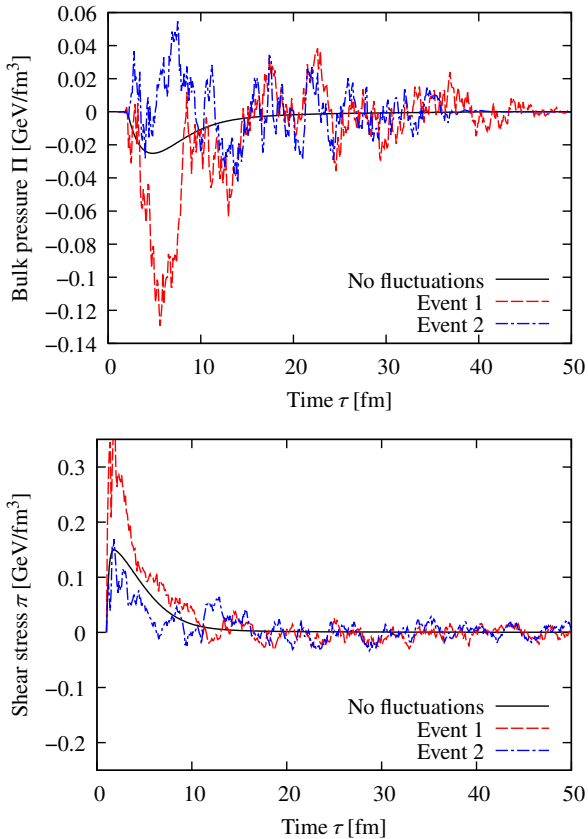


Figure 4: The time evolution of bulk pressure and shear stress are shown in the upper and lower panel, respectively. The results of dissipative hydrodynamics is shown by the black solid lines. The results of fluctuating hydrodynamics is shown by red dashed and blue chain lines each of which corresponds to those in Fig. 2.

the derivation of the SSFT (26) is still valid for the current numerical setup, so the relation (24) is the remaining key to check the SSFT.

To see if the relation (24) holds for the current setup, it is useful to calculate the following ratio:

$$R = \frac{2\langle\bar{\sigma}\rangle}{a^2 \cdot (\tau - \tau_i)}. \quad (36)$$

Here  $R = 1$  means the SSFT, and its deviation from unity measures the breaking of the SSFT. The time dependence of the ratio  $R$  is shown in Fig. 6 for each model of the relaxation time. The ratio has very small values at the initial stage,  $\tau - \tau_i \lesssim \tau_R$ , and then converges to a final value at the later stage,  $\tau - \tau_i \gg \tau_R$ , which is consistent with the SSFT (12). The ratio for the default relaxation time becomes finally  $R \sim 0.56$  which is significantly smaller than unity. To study what breaks the SSFT, the result can be compared to those of the other relaxation times: Both of the ratios for the other two relaxation times successfully converge to values close to unity, which means that the SSFT is approximately valid for these relaxation times. The differences of the default relaxation time and these relaxation times lie in the temperature dependence: The

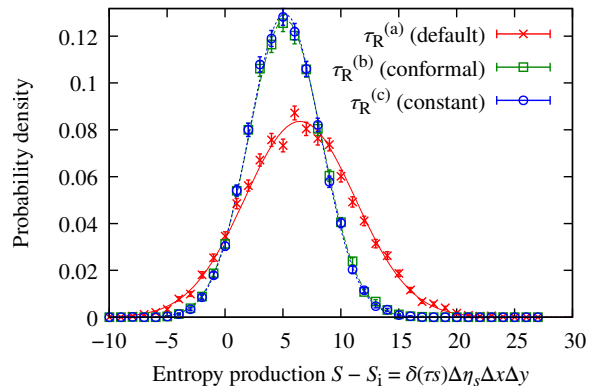


Figure 5: Probability distributions of entropy production in one fluid element at  $\tau = 50$  fm are shown for the three models of relaxation times. The error bars show statistical errors. The curves are fitted by Gaussian distributions.

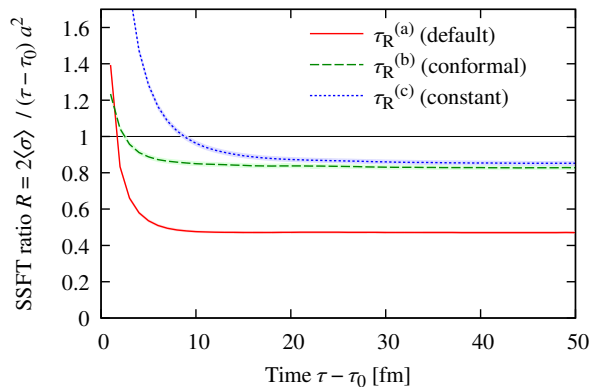


Figure 6: The SSFT ratio  $R$  is shown as a function of the time. Statistical errors are shown by bands.

default relaxation time peaks around the crossover temperature. The rapid variation of the relaxation time caused by this strong temperature dependence breaks the SSFT as we will see in the next section. This means that the SSFT ratio  $R$  is sensitive to the temperature dependence of the relaxation time.

## 6. SSFT breaking

In the previous section we observed breaking of the SSFT by numerical simulations. In this section, to get a deeper understanding, we discuss two effects that break the SSFT each of which corresponds to an idealised condition introduced in Sec. 3, *i.e.*, the effects of (i) background fluctuations caused by the hydrodynamic fluctuations and (ii) non-vanishing relaxation time.

### 6.1. Background fluctuations

Here we discuss the effects of temperature fluctuations numerically. We first obtain the evolution of non-fluctuating



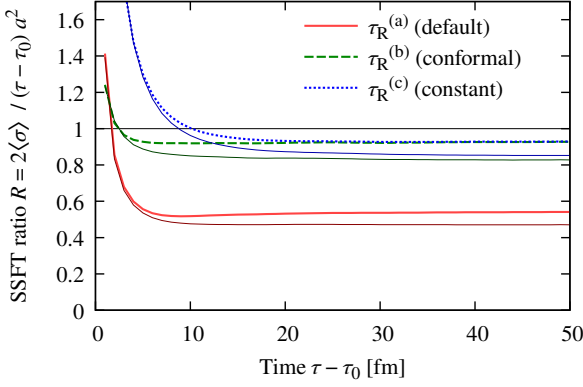


Figure 7: The SSFT ratios calculated under the non-fluctuating background  $T_0(\tau)$  are compared to those of the full non-linear time evolution shown in Fig. 6. The thick lines and thin solid lines correspond to the SSFT ratios under the non-fluctuating background and in the full time evolution, respectively. The red solid, green dashed and blue dotted lines represent the results for the three relaxation models, respectively.

background temperature,  $T_0(\tau)$ , by numerically solving Eqs. (7)–(9) without hydrodynamic fluctuations. Then we solve the constitutive equations (8) and (9) under the non-fluctuating background  $T_0(\tau)$  and finally perform event-by-event integrations of the entropy production (15). In Fig. 7, the time evolution of the SSFT ratio under the non-fluctuating background is compared to the full non-linear time evolution for each relaxation time model. One can observe that the corrections due to the fluctuating background are around  $\sim 0.1$  and have weak dependence on the relaxation time models.

## 6.2. Non-vanishing relaxation time

We next discuss effects of non-vanishing relaxation time under the non-fluctuating background evolution  $T_0(\tau)$ . We now consider the case  $\tau_\pi = \tau_\Pi = \tau_R$  following our numerical setup in the previous section. Combining Eqs. (15)–(20), the expression of entropy production is written as

$$\begin{aligned} \bar{\sigma} &= \frac{\Delta V}{\tau - \tau_i} \int_{\tau_i}^{\tau} \frac{d\tau_1}{T_0(\tau_1)} \int_{\tau_i}^{\tau_1} d\tau_2 G_0(\tau_1, \tau_2) F(\tau_2) \\ &= \frac{\Delta V}{\tau - \tau_i} \int_{\tau_i}^{\tau} d\tau_2 \int_{\tau_2}^{\tau} \frac{d\tau_1}{T_0(\tau_1)} G_0(\tau_1, \tau_2) F(\tau_2), \end{aligned} \quad (37)$$

where  $\Delta V = \Delta\eta_s \Delta x \Delta y$ ,  $F(\tau) = 3\eta_0(\tau)/4\tau + \zeta_0(\tau)/\tau + \xi_\pi(\tau) - \xi_\Pi(\tau)$ , and the integral kernel  $G_0(\tau_1, \tau_2)$  is defined using the background relaxation time  $\tau_{R0}(\tau) = \tau_R(T_0(\tau))$ . We then use the relation  $[1 + \tau_{R0}(\tau_1)d/d\tau_1]G_0(\tau_1, \tau_2) = 0$  to replace  $G_0(\tau_1, \tau_2)$  with  $-\tau_{R0}(\tau_1)(d/d\tau_1)G_0(\tau_1, \tau_2)$  and perform integration by parts with respect

to  $\tau_1$  to obtain the following expression:

$$\begin{aligned} \bar{\sigma} &= \frac{\Delta V}{\tau - \tau_i} \left[ \int_{\tau_i}^{\tau} d\tau_2 \frac{F(\tau_2)}{T_0(\tau_2)} \right. \\ &\quad - \frac{\tau_{R0}(\tau)}{T_0(\tau)} \int_{\tau_i}^{\tau} d\tau_2 G_0(\tau, \tau_2) F(\tau_2) \\ &\quad \left. + \int_{\tau_i}^{\tau} d\tau_1 \left( \frac{d}{d\tau_1} \frac{\tau_{R0}(\tau_1)}{T_0(\tau_1)} \right) \int_{\tau_i}^{\tau_1} d\tau_2 G_0(\tau_1, \tau_2) F(\tau_2) \right], \end{aligned} \quad (38)$$

where the first and second terms are obtained as surface terms. One notices that the first term is exactly the same as the expression in the Navier–Stokes limit (21) while the second and third terms are the corrections by the non-vanishing relaxation time. Specifically one can observe that the second and third terms have factors  $(\tau_R/T)$  and  $D(\tau_R/T)$ , respectively, and therefore they are identified to be the corrections due to the absolute value and the temporal change of the relaxation time, respectively.

The mean of entropy production is

$$\langle \bar{\sigma} \rangle = \frac{\Delta V}{\tau - \tau_i} \int_{\tau_i}^{\tau} \frac{d\tau_1}{T_0(\tau_1)} \int_{\tau_i}^{\tau_1} d\tau_2 G_0(\tau_1, \tau_2) \langle F(\tau_2) \rangle, \quad (39)$$

where  $\langle F(\tau) \rangle = 4\eta_0(\tau)/3\tau + \zeta_0(\tau)/\tau$ . The variance can be calculated by applying the FDR,  $\langle \delta F(\tau_1) \delta F(\tau_2) \rangle = 2T_0(\tau_1) \langle F(\tau_1) \rangle \delta(\tau_1 - \tau_2) / \Delta V$  with  $\delta F = F - \langle F \rangle$ , to the product of Eqs. (37) and (38). As a result we obtain three terms each of which corresponds to each term in Eq. (38):

$$a^2 = 2(\langle \bar{\sigma} \rangle + \gamma + \delta). \quad (40)$$

Here

$$\begin{aligned} \gamma &= -\frac{\Delta V}{\tau - \tau_i} \frac{\tau_{R0}(\tau)}{T(\tau)} \int_{\tau_i}^{\tau} \frac{d\tau_1}{T_0(\tau_1)} \\ &\quad \times \int_{\tau_i}^{\tau_1} d\tau_2 G_0(\tau, \tau_2) G_0(\tau_1, \tau_2) T_0(\tau_2) \langle F(\tau_2) \rangle, \end{aligned} \quad (41)$$

$$\begin{aligned} \delta &= \frac{\Delta V}{\tau - \tau_i} \int_{\tau_i}^{\tau} \frac{d\tau_1}{T_0(\tau_1)} \int_{\tau_i}^{\tau} \frac{d\tau_3}{T_0(\tau_3)} \left[ T_0(\tau_3) D_3 \frac{\tau_{R0}(\tau_3)}{T_0(\tau_3)} \right] \\ &\quad \times \int_{\tau_i}^{\tau_{\min}} d\tau_2 G_0(\tau_1, \tau_2) G_0(\tau_3, \tau_2) T_0(\tau_2) \langle F(\tau_2) \rangle, \end{aligned} \quad (42)$$

where  $D_3 = d/d\tau_3$  and  $\tau_{\min} = \min\{\tau_1, \tau_3\}$ .

Now we discuss the deviation of the SSFT ratio,  $R$ , from unity. The inverse ratio is obtained from Eq. (40):

$$R^{-1} = 1 + \frac{\gamma}{\langle \bar{\sigma} \rangle} + \frac{\delta}{\langle \bar{\sigma} \rangle}. \quad (43)$$

First we discuss the second term  $\gamma$ . One can observe in Eq. (41) that it contains an explicit  $\tau_{R0}$  dependence only outside of the integration, and therefore the term is considered to be the correction to  $R$  solely due to the finiteness of the relaxation time. The third term  $\delta$  is considered to be the correction due to the temporal change of the relaxation time as one can see that it is proportional to a



dimensionless factor  $TD(\tau_R/T)$  in Eq. (42). From magnitudes of the two terms in  $TD(\tau_R/T) = D\tau_R - (\tau_R/T)DT$ , the conditions for the vanishing third term read:

$$D\tau_R \ll 1, \quad (44)$$

$$\tau_R \ll 1/(D \ln T). \quad (45)$$

The second condition implies that the relaxation time should be sufficiently shorter than the hydrodynamic time scale of temperature change. The first condition can be interpreted similarly: The relaxation time should be shorter than the variation time scale of the relaxation time itself since the condition can be rewritten as  $\tau_R \ll 1/(D \ln \tau_R)$ . The large deviation of  $R$  from unity with the relaxation time model  $\tau_R^{(a)}$  in Fig. 6 can be understood by this effect. The relaxation time  $\tau_R^{(a)}(T)$  have a peak structure in its temperature dependence, so it changes rapidly in the time evolution to break the condition  $D\tau_R \ll 1$ . For the other relaxation time models, the temporal change of  $\tau_R$  is milder, which explains their smaller deviation of  $R$  from unity.

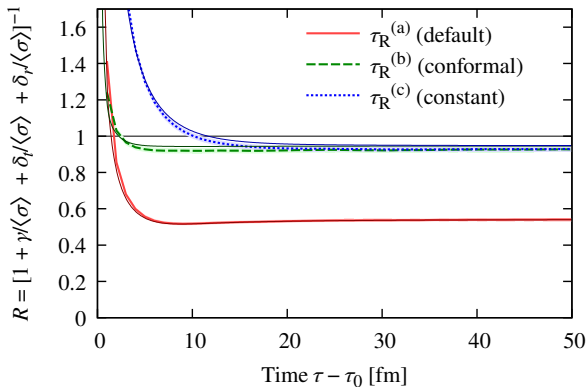


Figure 8: The SSFT ratios evaluated by numerical integrations of the analytic expressions (39), (41) and (42) are compared to those by the numerical simulations under the non-fluctuating background  $T_0(\tau)$  shown in Fig. 8. The thin solid lines and thick lines represent the results for the analytic expressions and the event-by-event numerical simulations, respectively. The red, green and blue lines correspond to the results for the three relaxation models, respectively. The bands with pale colours show the statistical errors of the results of the numerical simulations.

To quantify the effects of each correction we perform numerical integrations of these analytic expressions (39), (41) and (42). In particular we separate two different contributions from  $\delta$  corrections,  $\delta = \delta_t + \delta_r$ , where the temperature evolution effect  $\delta_t$  and the relaxation time evolution effect  $\delta_r$  correspond to the two terms in  $TD(\tau_R/T) = -(\tau_R/T^2)DT + D\tau_R$ , respectively. For an efficient evaluation of the time dependence of the integrations, we construct dynamical equations of the integrals (See Appendix C). Figure 8 shows the time dependence of the SSFT ratio evaluated by numerical integration of the analytic expressions compared to the results by the event-by-event numerical simulations under the non-fluctuating background

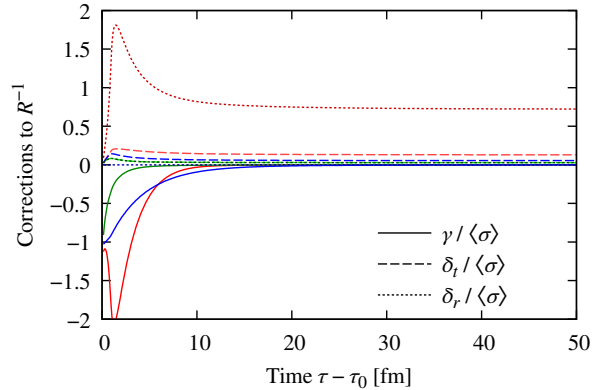


Figure 9: The corrections to the SSFT factor  $R$  are shown. The solid, dashed and dotted line represent the corrections due to the finiteness of the relaxation time  $\gamma$ , the temperature evolution  $\delta_t$  and the relaxation time evolution  $\delta_r$ , respectively. The red, green and blue lines correspond to the results for the three relaxation models, respectively, as the same as the other figures.

$T_0(\tau)$ . One can see that the results of the event-by-event numerical simulations are reproduced by the analytic expressions within statistical errors.

Figure 9 shows the time dependence of each correction to the SSFT factor  $R$ . One can see that the corrections  $\gamma$  shown by solid lines vanish within 10–20 fm, and therefore the remaining contributions at the final time are only  $\delta_t$  and  $\delta_r$ . The corrections  $\delta_t$  shown by dashed lines have relatively the same order of contributions while the corrections  $\delta_r$  shown by dotted lines have dramatic differences among the relaxation time models. The  $\delta_r$  correction for the constant relaxation time model shown by blue dotted line trivially vanishes since the relaxation time does not change in this model. The  $\delta_r$  correction for the conformal relaxation time model shown by green dotted line has exactly the same value with the  $\delta_t$  corrections since in this model the two terms from  $D(\tau_R/T) = (1/T)D\tau_R + \tau_R D(1/T)$  give the identical contributions as  $\tau_R \propto 1/T$ . The  $\delta_r$  correction for the default model shown by red dotted line gives a large correction because of the fast evolution of the relaxation time explained by the steep temperature dependence of the relaxation time around the crossover region.

Thus the significant deviation of the SSFT ratio  $R$  of the default relaxation model in Fig. 6 was quantitatively confirmed to be the  $\delta_r$  correction, the correction due to the time evolution of the relaxation time. The remaining deviations are explained by the time evolution of the temperature and the background fluctuations.

## 7. Summary and concluding remarks

In this paper we focused on the distribution of entropy production caused by the hydrodynamic fluctuations, *i.e.*, the thermal fluctuations of hydrodynamics, in a simple setup of the Bjorken flow which is a one-dimensionally expanding system. The dynamics of the system is described

by the relativistic fluctuating hydrodynamics whose equations become stochastic differential equations due to the noise terms. In (i) a limit that the considered fluid element is large enough that the background fluctuations are negligible and (ii) the Navier–Stokes limit where the relaxation time is sufficiently shorter than the time scale of macroscopic dynamics of hydrodynamic fields, we have shown a relation in the expanding system (24) which shares the same structure with the SSFT (12). As a consequence of this “SSFT” in the Bjorken expansion, we have also shown an inequality (30) between the initial entropy and the relative fluctuations of the final entropy. The consequence to the experimental observables of high-energy nuclear collisions is the inequality on the multiplicity (31) where the left-hand side of the inequality can be directly measured in experiments, and the right-hand side is determined solely by the initial condition models independently from the intermediate dynamics of the system. We also pointed out that the multiplicity fluctuations are more significant in the smaller collision systems as is the common nature of the thermal fluctuations.

In realistic modeling of the high-energy nuclear collisions by the second-order causal viscous hydrodynamics, the relaxation time is comparable to the time scale of the hydrodynamics. In addition there would be the effects from the background fluctuations, so we have numerically checked the breaking of the SSFT by those effects by defining the ratio  $R$  (36) from the SSFT (24). We performed (0+1)-dimensional event-by-event simulations of relativistic fluctuating hydrodynamics in the Bjorken expansion using a stochastic Runge–Kutta method and obtained the distribution of the final entropy production. As a result we found that the breaking of the SSFT is more significant for the relaxation time model that has strong temperature dependence. To understand the result, we have analytically investigated what effects break the SSFT with non-vanishing relaxation times and identified three different contributions: the finiteness of the relaxation time, the temperature evolution and the relaxation time evolution. The first effect vanishes in a time scale of the relaxation time, and the second effect is relatively independent of the relaxation time model. The third effect largely depends on the relaxation time models. We also checked the effects of background fluctuations by performing the event-by-event simulations using the non-fluctuating background temperature evolution.

As a future work we are now preparing to investigate the effects of the FDR corrections in non-static and inhomogeneous background in detail. Also, in the present analysis, we assumed the Bjorken flow which means that the fluctuations of the flow velocity are not considered in the analysis. The effects of the flow fluctuations to the SSFT would be one of the future tasks. Another interesting topic is about the definition of the entropy. In defining the entropy production, we employed the equilibrium entropy  $s$  but not the non-equilibrium entropy of the second-order hydrodynamics,  $s_{\text{neq}} = s - \tau_{\Pi} \Pi^2 / 2T\zeta - \tau_{\pi} \pi^2 / 4T\eta$ . In fact

the SSFT does not seem to be reproduced for the non-equilibrium entropy in our present numerical calculations and analytical studies, but its detailed understanding and interpretation is another future task.

## Acknowledgments

The authors thank Tomoi Koide for useful discussions. The work of T. H. was supported by JSPS KAKENHI Grant No. JP17H02900.

## Appendix A. Multiplicity fluctuations

In this section we derive the upper bound of the multiplicity fluctuations in Eq. (31). To calculate the multiplicity fluctuations we should distinguish three different fluctuations: (1) initial entropy fluctuations originating from initial state fluctuations, (2) the hydrodynamic fluctuations on which we focus in this paper and (3) the particle number fluctuations which appear when we switch the system description from thermodynamic fields to hadrons using the Cooper–Frye formula [34]. To deal with these fluctuations we define three corresponding averages: (1)  $\langle O \rangle_{\text{IS}}$  is the average over different initial conditions, (2)  $\langle O \rangle_{\xi}$  is the average over different noise processes for a fixed initial entropy  $S_{\text{tot},i}$ , and (3)  $\langle O \rangle_{\text{CF}}$  is the average over particle number fluctuations by the Cooper–Frye sampling for a fixed final entropy. The event average can be expressed as  $\langle O \rangle_{\text{ev}} = \langle \langle O \rangle_{\text{CF}} \rangle_{\xi} \rangle_{\text{IS}}$ .

With this terminology Eq. (30) is rewritten as

$$\frac{\langle (S_{\text{tot}} - \langle S_{\text{tot}} \rangle_{\xi})^2 \rangle_{\xi}}{\langle S_{\text{tot}} \rangle_{\xi}^2} \leq \frac{1}{2S_{\text{tot},i}}. \quad (\text{A.1})$$

Then we take the averages over initial conditions:

$$\langle \langle (S_{\text{tot}} - \langle S_{\text{tot}} \rangle_{\xi})^2 \rangle_{\xi} \rangle_{\text{IS}} \leq \left\langle \frac{\langle S_{\text{tot}} \rangle_{\xi}^2}{2S_{\text{tot},i}} \right\rangle_{\text{IS}}. \quad (\text{A.2})$$

The left-hand side is decomposed into two parts as

$$\begin{aligned} & \langle \langle (S_{\text{tot}} - \langle S_{\text{tot}} \rangle_{\xi})^2 \rangle_{\xi} \rangle_{\text{IS}} \\ &= \langle [(S_{\text{tot}} - \langle S_{\text{tot}} \rangle_{\text{ev}}) - (\langle S_{\text{tot}} \rangle_{\xi} - \langle S_{\text{tot}} \rangle_{\text{ev}})]^2 \rangle_{\text{ev}} \\ &= (\Delta_{\text{ev}} S_{\text{tot}})^2 - \langle \langle (S_{\text{tot}} \rangle_{\xi} - \langle S_{\text{tot}} \rangle_{\text{ev}})^2 \rangle_{\text{ev}}, \end{aligned} \quad (\text{A.3})$$

where  $(\Delta_{\text{ev}} S_{\text{tot}})^2 = \langle (S_{\text{tot}} - \langle S_{\text{tot}} \rangle_{\text{ev}})^2 \rangle_{\text{ev}}$ . We used  $\langle f(S_{\text{tot}}) \rangle_{\text{ev}} = \langle \langle f(S_{\text{tot}}) \rangle_{\xi} \rangle_{\text{IS}}$  which comes from the fact that  $S_{\text{tot}}$  is independent of the particle number fluctuations, *i.e.*,  $\langle S_{\text{tot}} \rangle_{\text{CF}} = S_{\text{tot}}$ . The right-hand side is transformed as

$$\begin{aligned} \left\langle \frac{\langle S_{\text{tot}} \rangle_{\xi}^2}{2S_{\text{tot},i}} \right\rangle_{\text{IS}} &= \left\langle \frac{\langle S_{\text{tot}} \rangle_{\xi}}{2} \cdot \frac{\langle S_{\text{tot}} \rangle_{\text{ev}}}{\langle S_{\text{tot},i} \rangle_{\text{ev}}} \right\rangle_{\text{IS}} \\ &= \frac{\langle S_{\text{tot}} \rangle_{\text{ev}}^2}{2\langle S_{\text{tot},i} \rangle_{\text{ev}}}, \end{aligned} \quad (\text{A.4})$$

where we used the relation,  $\langle S_{\text{tot}} \rangle_{\xi} / S_{\text{tot},i} = \langle S_{\text{tot}} \rangle_{\text{ev}} / \langle S_{\text{tot},i} \rangle_{\text{ev}} = \text{const}$ , coming from the assumption that both of  $\langle S_{\text{tot}} \rangle_{\xi}$

and  $S_{\text{tot},i}$  are proportional to the transverse area  $A$  of each initial condition. Plugging them into Eq. (A.2), we obtain the upper bound of the relative fluctuations of the final entropy with initial fluctuations considered:

$$\begin{aligned} \frac{(\Delta_{\text{ev}} S_{\text{tot}})^2}{\langle S_{\text{tot}} \rangle_{\text{ev}}^2} &\leq \frac{\langle (\langle S_{\text{tot}} \rangle_{\xi} - \langle S_{\text{tot}} \rangle_{\text{ev}})^2 \rangle_{\text{ev}}}{\langle S_{\text{tot}} \rangle_{\text{ev}}^2} + \frac{1}{2\langle S_{\text{tot},i} \rangle_{\text{ev}}} \\ &= \frac{(\Delta_{\text{ev}} S_{\text{tot},i})^2}{\langle S_{\text{tot},i} \rangle_{\text{ev}}^2} + \frac{1}{2\langle S_{\text{tot},i} \rangle_{\text{ev}}}. \end{aligned} \quad (\text{A.5})$$

To obtain the second line we again used the relation,  $\langle S_{\text{tot}} \rangle_{\xi} \propto S_{\text{tot},i} \propto A$ .

Next we will relate the entropy fluctuations to the multiplicity fluctuations. Since we assumed the Poisson distribution for the particlisation, the mean and variance of the multiplicity for a fixed final entropy becomes  $\langle N \rangle_{\text{CF}} = \langle (N - \langle N \rangle_{\text{CF}})^2 \rangle_{\text{CF}} = \alpha S_{\text{tot}}$  with  $\alpha$  being a proportionality constant. Using this relation we obtain the multiplicity fluctuations as follows:

$$\begin{aligned} \frac{\langle (N - \langle N \rangle_{\text{ev}})^2 \rangle_{\text{ev}}}{\langle N \rangle_{\text{ev}}^2} &= \frac{\langle [(N - \langle N \rangle_{\text{CF}}) + (\langle N \rangle_{\text{CF}} - \langle N \rangle_{\text{ev}})]^2 \rangle_{\text{ev}}}{\langle N \rangle_{\text{ev}}^2} \\ &= \frac{\langle (N - \langle N \rangle_{\text{CF}}) \rangle_{\text{ev}}}{\langle N \rangle_{\text{ev}}^2} + \frac{\langle (\langle N \rangle_{\text{CF}} - \langle N \rangle_{\text{ev}})^2 \rangle_{\text{ev}}}{\langle N \rangle_{\text{ev}}^2} \\ &= \frac{(\Delta_{\text{ev}} S_{\text{tot}})^2}{\langle S_{\text{tot}} \rangle_{\text{ev}}^2} + \frac{1}{\langle N \rangle_{\text{ev}}}. \end{aligned} \quad (\text{A.6})$$

Combining Eqs. (A.5) and (A.6), we obtain Eq. (31). Finally we note that, as the origin of the hydrodynamic fluctuations is the microscopic degrees of freedom, a part of the particlisation fluctuations may be already contained in the hydrodynamic fluctuations. Nevertheless, the inequality is still valid since in such a case the upper bound is just overestimated.

## Appendix B. Stochastic Runge–Kutta method

In our numerical simulations we used a second-order stochastic Runge–Kutta method for the Stratonovich stochastic differential equations. Our equations of fluctuating hydrodynamics in one-dimensionally expanding systems can be summarized in the following structure:

$$DX_i(\tau) = f_i(\tau, \vec{X}(\tau)) + \sum_a g_{ia}(\tau, \vec{X}(\tau)) \circ w_a(\tau), \quad (\text{B.1})$$

where  $D = d/d\tau$  is the time derivative,  $\vec{X}(\tau) = \{X_i(\tau)\}_i$  is the set of dynamical variables, and  $\{w_a(\tau)\}_a$  are the noise terms satisfying the normalization  $\langle w_a(\tau) w_b(\tau') \rangle = \delta_{ab} \delta(\tau - \tau')$ . The coefficients,  $f_i(\tau, \vec{X})$  and  $g_{ia}(\tau, \vec{X})$ , are the average and fluctuating parts of the time derivatives, respectively. In the stochastic Runge–Kutta method, which we employed, one calculates the next-step state,  $X_i^{(n+1)} =$

$X_i(\tau_{n+1} = \tau_n + \Delta\tau)$ , from the previous-step state,  $X_i^{(n)} = X_i(\tau_n)$ , using the following equations:

$$\begin{aligned} K_i^{(1)} &= f_i(\tau_n, \vec{X}^{(n)}) \Delta\tau \\ &+ \sum_a g_{ia}(\tau_n, \vec{X}^{(n)}) \Delta W_a, \end{aligned} \quad (\text{B.2})$$

$$\begin{aligned} K_i^{(2)} &= X_i^{(n)} + f_i(\tau_{n+1}, \vec{X}^{(n)} + \vec{K}^{(1)}) \Delta\tau \\ &+ \sum_a g_{ia}(\tau_{n+1}, \vec{X}^{(n)} + \vec{K}^{(1)}) \Delta W_a, \end{aligned} \quad (\text{B.3})$$

$$X_i^{(n+1)} = X_i^{(n)} + \frac{1}{2}(K_i^{(1)} + K_i^{(2)}), \quad (\text{B.4})$$

where  $\{\Delta W_a\}_a$  are independent Gaussian random numbers of the standard deviation  $\sqrt{\Delta\tau}$ .

## Appendix C. Numerical integration of analytic corrections

Here we describe an efficient way to evaluate the time dependence of the analytic corrections  $\gamma$ ,  $\delta_t$  and  $\delta_r$ . First we transform the expressions as follows:

$$\gamma(\tau) = -\frac{\Delta V}{2(\tau - \tau_i)} \frac{\tau_{\text{R0}}(\tau)}{T_0(\tau)} I(\tau), \quad (\text{C.1})$$

$$\delta_a(\tau) = \frac{\Delta V}{2(\tau - \tau_i)} \Delta_a(\tau), \quad (\text{C.2})$$

$$\Delta_a(\tau) = \int_{\tau_i}^{\tau} \frac{d\tau_1}{T_0(\tau_1)} I_a(\tau_1) + \int_{\tau_i}^{\tau} d\tau_3 D_a(\tau_3) I(\tau_3), \quad (\text{C.3})$$

$$I(\tau) = \int_{\tau_i}^{\tau} d\tau_1 G_0(\tau, \tau_1) \frac{\tau_{\text{R0}}(\tau_1)}{T_0(\tau_1)} \Gamma(\tau_1), \quad (\text{C.4})$$

$$I_a(\tau) = \int_{\tau_i}^{\tau} d\tau_3 G_0(\tau, \tau_3) \tau_{\text{R0}}(\tau_3) D_a(\tau_3) \Gamma(\tau_3), \quad (\text{C.5})$$

$$\Gamma(\tau) = \int_{\tau_i}^{\tau} d\tau_1 G_{1/2}(\tau, \tau_1) \frac{T_0(\tau_1)}{\tau_{\text{R0}}(\tau_1)} \langle F(\tau_1) \rangle, \quad (\text{C.6})$$

where the subscript  $a$  is either  $t$  or  $r$ ,  $D_t(\tau) = \tau_{\text{R0}}(\tau) D(1/T_0(\tau))$  and  $D_r(\tau) = (1/T_0(\tau)) D\tau_{\text{R0}}(\tau)$ . The function  $G_{1/2}(\tau, \tau_1)$  is the Green function of the ‘‘half relaxation time’’ defined as

$$\begin{aligned} G_{1/2}(\tau, \tau_1) &= 2G_0(\tau, \tau_1)^2 \tau_{\text{R0}}(\tau_1) \\ &= \exp\left(-\int_{\tau_1}^{\tau} \frac{d\tau'}{\tau_{\text{R0}}(\tau')/2}\right) \frac{1}{\tau_{\text{R0}}(\tau_1)/2}. \end{aligned} \quad (\text{C.7})$$

Then we find the following differential equations for the above integrations:

$$\left[1 + \frac{\tau_{\text{R0}}(\tau)}{2} D\right] \Gamma(\tau) = \frac{T_0(\tau)}{\tau_{\text{R0}}(\tau)} \langle F(\tau) \rangle, \quad (\text{C.8})$$

$$[1 + \tau_{\text{R0}}(\tau) D] I(\tau) = \frac{\tau_{\text{R0}}(\tau)}{T_0(\tau)} \Gamma(\tau), \quad (\text{C.9})$$

$$[1 + \tau_{\text{R0}}(\tau) D] I_a(\tau) = \tau_{\text{R0}}(\tau) D_a(\tau) \Gamma(\tau), \quad (\text{C.10})$$

$$D\Delta_a = \frac{1}{T_0(\tau)} I_a(\tau) + D_a(\tau) I(\tau). \quad (\text{C.11})$$

Starting from the initial conditions  $\Gamma(\tau_i) = I(\tau_i) = I_a(\tau_i) = \Delta_a(\tau_i) = 0$ , one can solve these equations to obtain the time dependence of corrections using such as the Runge–Kutta methods.

## References

- [1] P. F. Kolb, J. Sollfrank, U. W. Heinz, Anisotropic transverse flow and the quark hadron phase transition, *Phys. Rev. C* 62 (2000) 054909. [arXiv:hep-ph/0006129](#), [doi:10.1103/PhysRevC.62.054909](#).
- [2] D. Teaney, J. Lauret, E. V. Shuryak, Flow at the SPS and RHIC as a quark gluon plasma signature, *Phys. Rev. Lett.* 86 (2001) 4783–4786. [arXiv:nucl-th/0011058](#), [doi:10.1103/PhysRevLett.86.4783](#).
- [3] T. Hirano, K. Tsuda, Collective flow and two pion correlations from a relativistic hydrodynamic model with early chemical freezeout, *Phys. Rev. C* 66 (2002) 054905. [arXiv:nucl-th/0205043](#), [doi:10.1103/PhysRevC.66.054905](#).
- [4] P. Romatschke, U. Romatschke, Viscosity Information from Relativistic Nuclear Collisions: How Perfect is the Fluid Observed at RHIC?, *Phys. Rev. Lett.* 99 (2007) 172301. [arXiv:0706.1522](#), [doi:10.1103/PhysRevLett.99.172301](#).
- [5] H. Song, S. A. Bass, U. Heinz, T. Hirano, C. Shen, 200 A GeV Au+Au collisions serve a nearly perfect quark-gluon liquid, *Phys. Rev. Lett.* 106 (2011) 192301, [Erratum: *Phys. Rev. Lett.* 109,139904(2012)]. [arXiv:1011.2783](#), [doi:10.1103/PhysRevLett.106.192301](#), [doi:10.1103/PhysRevLett.109.139904](#).
- [6] M. Luzum, P. Romatschke, Conformal Relativistic Hydrodynamics: Applications to RHIC results at  $\sqrt{s_{NN}} = 200$ -GeV, *Phys. Rev. C* 78 (2008) 034915, [Erratum: *Phys. Rev. C* 79,039903(2009)]. [arXiv:0804.4015](#), [doi:10.1103/PhysRevC.78.034915](#), [doi:10.1103/PhysRevC.79.039903](#).
- [7] H. Song, U. W. Heinz, Extracting the QGP viscosity from RHIC data - A Status report from viscous hydrodynamics, *J. Phys. G* 36 (2009) 064033. [arXiv:0812.4274](#), [doi:10.1088/0954-3899/36/6/064033](#).
- [8] B. Schenke, S. Jeon, C. Gale, Anisotropic flow in  $\sqrt{s} = 2.76$  TeV Pb+Pb collisions at the LHC, *Phys. Lett. B* 702 (2011) 59–63. [arXiv:1102.0575](#), [doi:10.1016/j.physletb.2011.06.065](#).
- [9] A. Adare, et al., Measurements of Higher-Order Flow Harmonics in Au+Au Collisions at  $\sqrt{s_{NN}} = 200$  GeV, *Phys. Rev. Lett.* 107 (2011) 252301. [arXiv:1105.3928](#), [doi:10.1103/PhysRevLett.107.252301](#).
- [10] P. Sorensen, Higher Flow Harmonics in Heavy Ion Collisions from STAR, *J. Phys. G* 38 (2011) 124029. [arXiv:1110.0737](#), [doi:10.1088/0954-3899/38/12/124029](#).
- [11] K. Aamodt, et al., Higher harmonic anisotropic flow measurements of charged particles in Pb-Pb collisions at  $\sqrt{s_{NN}} = 2.76$  TeV, *Phys. Rev. Lett.* 107 (2011) 032301. [arXiv:1105.3865](#), [doi:10.1103/PhysRevLett.107.032301](#).
- [12] G. Aad, et al., Measurement of the azimuthal anisotropy for charged particle production in  $\sqrt{s_{NN}} = 2.76$  TeV lead-lead collisions with the ATLAS detector, *Phys. Rev. C* 86 (2012) 014907. [arXiv:1203.3087](#), [doi:10.1103/PhysRevC.86.014907](#).
- [13] S. Chatrchyan, et al., Centrality dependence of dihadron correlations and azimuthal anisotropy harmonics in PbPb collisions at  $\sqrt{s_{NN}} = 2.76$  TeV, *Eur. Phys. J. C* 72 (2012) 2012. [arXiv:1201.3158](#), [doi:10.1140/epjc/s10052-012-2012-3](#).
- [14] B. Alver, G. Roland, Collision geometry fluctuations and triangular flow in heavy-ion collisions, *Phys. Rev. C* 81 (2010) 054905, [Erratum: *Phys. Rev. C* 82,039903(2010)]. [arXiv:1003.0194](#), [doi:10.1103/PhysRevC.82.039903](#), [doi:10.1103/PhysRevC.81.054905](#).
- [15] M. A. Stephanov, K. Rajagopal, E. V. Shuryak, Signatures of the tricritical point in QCD, *Phys. Rev. Lett.* 81 (1998) 4816–4819. [arXiv:hep-ph/9806219](#), [doi:10.1103/PhysRevLett.81.4816](#).
- [16] M. A. Stephanov, K. Rajagopal, E. V. Shuryak, Event-by-event fluctuations in heavy ion collisions and the QCD critical point, *Phys. Rev. D* 60 (1999) 114028. [arXiv:hep-ph/9903292](#), [doi:10.1103/PhysRevD.60.114028](#).
- [17] K. Murase, T. Hirano, Relativistic fluctuating hydrodynamics with memory functions and colored noises [arXiv:1304.3243](#).
- [18] J. D. Bjorken, Highly Relativistic Nucleus-Nucleus Collisions: The Central Rapidity Region, *Phys. Rev. D* 27 (1983) 140–151. [doi:10.1103/PhysRevD.27.140](#).
- [19] R. Kubo, Statistical mechanical theory of irreversible processes. I. General theory and simple applications in magnetic and conduction problems, *J. Phys. Soc. Jap.* 12 (1957) 570–586. [doi:10.1143/JPSJ.12.570](#).
- [20] D. J. Evans, E. G. D. Cohen, G. P. Morriss, Probability of second law violations in shearing steady states, *Phys. Rev. Lett.* 71 (1993) 2401–2404. [doi:10.1103/PhysRevLett.71.2401](#). URL <https://link.aps.org/doi/10.1103/PhysRevLett.71.2401>
- [21] G. Gallavotti, E. G. D. Cohen, Dynamical ensembles in nonequilibrium statistical mechanics, *Phys. Rev. Lett.* 74 (1995) 2694–2697. [doi:10.1103/PhysRevLett.74.2694](#). URL <https://link.aps.org/doi/10.1103/PhysRevLett.74.2694>
- [22] D. J. Evans, D. J. Searles, Steady states, invariant measures, and response theory, *Phys. Rev. E* 52 (1995) 5839–5848. [doi:10.1103/PhysRevE.52.5839](#). URL <https://link.aps.org/doi/10.1103/PhysRevE.52.5839>
- [23] W. A. Hiscock, L. Lindblom, Stability and causality in dissipative relativistic fluids, *Annals Phys.* 151 (1983) 466–496. [doi:10.1016/0003-4916\(83\)90288-9](#).
- [24] W. A. Hiscock, L. Lindblom, Generic instabilities in first-order dissipative relativistic fluid theories, *Phys. Rev. D* 31 (1985) 725–733. [doi:10.1103/PhysRevD.31.725](#).
- [25] Y. Aoki, Z. Fodor, S. D. Katz, K. K. Szabo, The Equation of state in lattice QCD: With physical quark masses towards the continuum limit, *JHEP* 01 (2006) 089. [arXiv:hep-lat/0510084](#), [doi:10.1088/1126-6708/2006/01/089](#).
- [26] Y. Aoki, G. Endrodi, Z. Fodor, S. D. Katz, K. K. Szabo, The Order of the quantum chromodynamics transition predicted by the standard model of particle physics, *Nature* 443 (2006) 675–678. [arXiv:hep-lat/0611014](#), [doi:10.1038/nature05120](#).
- [27] A. Bazavov, et al., Equation of state and QCD transition at finite temperature, *Phys. Rev. D* 80 (2009) 014504. [arXiv:0903.4379](#), [doi:10.1103/PhysRevD.80.014504](#).
- [28] M. Asakawa, T. Hatsuda, What thermodynamics tells about QCD plasma near phase transition, *Phys. Rev. D* 55 (1997) 4488–4491. [arXiv:hep-ph/9508360](#), [doi:10.1103/PhysRevD.55.4488](#).
- [29] G. Policastro, D. T. Son, A. O. Starinets, The Shear viscosity of strongly coupled  $N=4$  supersymmetric Yang-Mills plasma, *Phys. Rev. Lett.* 87 (2001) 081601. [arXiv:hep-th/0104066](#), [doi:10.1103/PhysRevLett.87.081601](#).
- [30] S. Weinberg, Entropy generation and the survival of protogalaxies in an expanding universe, *Astrophys. J.* 168 (1971) 175. [doi:10.1086/151073](#).
- [31] H. Grad, On the kinetic theory of rarefied gases, *Communications on Pure and Applied Mathematics* 2 (4) (1949) 331–407. [arXiv:https://onlinelibrary.wiley.com/doi/pdf/10.1002/cpa.3160020403](#), [doi:10.1002/cpa.3160020403](#). URL <https://onlinelibrary.wiley.com/doi/abs/10.1002/cpa.3160020403>
- [32] I. Müller, Zum paradoxon der wärmeleitungstheorie, *Zeitschrift für Physik* 198 (4) (1967) 329–344. [doi:10.1007/BF01326412](#). URL <https://doi.org/10.1007/BF01326412>
- [33] W. Israel, J. Stewart, Transient relativistic thermodynamics and kinetic theory, *Annals of Physics* 118 (2) (1979) 341 – 372. [doi:https://doi.org/10.1016/0003-4916\(79\)90130-1](#). URL <http://www.sciencedirect.com/science/article/pii/0003491679901301>
- [34] F. Cooper, G. Frye, Comment on the Single Particle Distribution in the Hydrodynamic and Statistical Thermodynamic Models of Multiparticle Production, *Phys. Rev. D* 10 (1974) 186. [doi:10.1103/PhysRevD.10.186](#).